EasyChair Preprint

№ 1954

Optimization of Process Parameters in Electrohydraulic Forming using Taguchi Method

Archit Shrivastava, Meraj Ahmed and Digavalli Ravi Kumar

November 14, 2019

ISME

"Optimization of Process Parameters in Electrohydraulic Forming using Taguchi Method"

Archit Shrivastava [1*], Meraj Ahmed[2], D Ravi kumar [1],

[1] Department of Mechanical Engineering, Indian Institute of Technology Delhi, New Delhi-110016, India

[2] CSIR-Advanced Materials and Processes Research Institute, Bhopal-462024, India

*Corresponding author: shrivastava_archit@yahoo.com

Abstract: *The high velocity forming has emerged as a new technique due to certain advantages over conventional forming, especially for materials like Al, Cu, Mg and their alloys. Electrohydraulic forming (EHF) is one such process where very high strain rates in the range of 10^2 to 10^5 /sec are applied during forming. In this process, a copper wire connecting two electrodes of a capacitor bank is fused to release a very high amount of energy in very short span of time. The fusing of the wire creates a shock wave which suddenly raises the pressure inside the chamber that is utilized to deform the blank into the die. The effect of important process parameters such as Stand-off distance, Electrode Gap, Voltage and Medium on formability has been studied in the present work. Optimization of these parameters has been carried out using Taguchi method for a commercially pure aluminum sheet in simple free bulging (biaxial stretching). Experiments have been performed based on the Taguchi's L9 orthogonal array. The optimum process parameters have been identified for the maximum dome height. The individual contribution of process parameters has also been determined.*

Keywords: Electrohydraulic forming, Aluminum, Sheet metal forming, Taguchi method, Optimization

1. Introduction

Among the high Energy rate forming (HERF) or high strain rate forming processes Electromagnetic forming (EMF) and Electrohyraulic forming (EHF) have received high attraction of the researchers in the recent past for applications in sheet metal forming industry. In these processes strain rates are in the range of 10^2 to 10^5 /sec and the velocity of the deforming sheet is more than 5m/sec. The high strain rate forming process works on the principle of pulse forming as the energy is delivered in a very short span of time i.e. in microsecond [1, 2]. Unlike in conventional forming where rigid tool are used to apply the force mechanically, techniques like repulsive force in case of EMF [3] , fusion of wire or spark in medium gap between electrodes in case of EHF [4, 5] and detonation of an explosive in case of explosive forming are used to deform the sheet metal [6]. EMF process can be used to form the material having good conductivity only [7] and explosive forming has limited use because of risks involved in handling and usage of explosives.

In view of this, EHF process has gained significance very rapidly in recent times as it combines the advantages of high strain rate forming and hydroforming. EHF is a process in which high voltage discharge of capacitors between two electrodes positioned in a fluid (water or oil) filled chamber. Electrodes are joined by copper wire as shown in Figure 1(a). Capacitor bank delivers a pulse of high current across two electrodes. The copper wire gets exploded, which creates shock wave in the fluid. The shock wave deforms the blank into a die as shown in Figure 1(b). The product formed by this process has high surface finish as it is a non-contact process and also no lubrication is required. It increases the formability of the material and decreases springback and wrinkling [7]. The process is very fast in nature and leads to very high productivity with some automation [1].

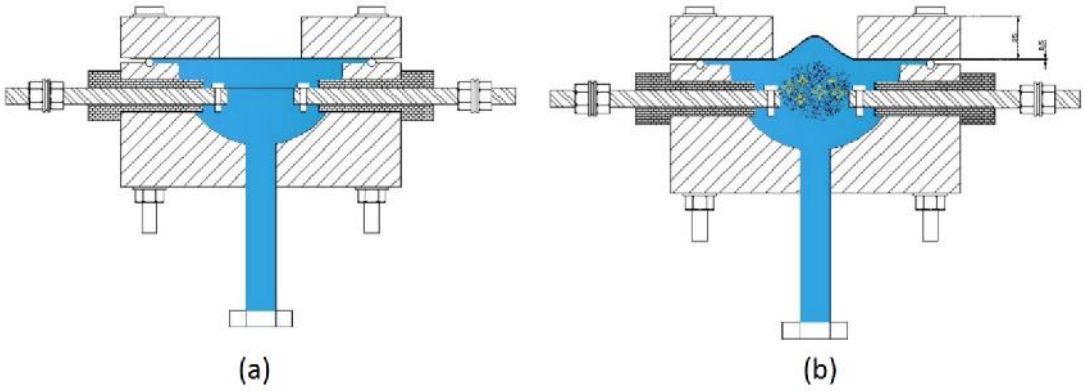

Figure 1: Chamber assembly with electrodes and free forming die (a) before energy supply (b) after energy supply

The initial work focused on demonstration of the process and outlining the principles of the same Yutin et. al. [8] discussed the bulging of tubes using successive electrical discharges. The use of fusing wire or initiating wire connected between the electrodes has been reported by Wesley et al. [9]. Schwinghamer et al. [10] discussed the comparative study on EHF and Electromagnetic forming process. Gilchrist et al. [11] reported EHF as explosive forming by underwater electrical discharge. Loeffler et al. [5] showed that the electrical wire explosion can be used as an alternative for other blasting processes. The electrical wire was exploded by passing very high energy in a very short time. Farzin et al. [12] carried out a comparative study between Viscous pressure forming (VPF) and EHF. Various miniature parts of good quality were produced by VPF and EHF process. The effect of stand-off distance and thickness of the sheet on the part quality was also discussed. Rohatgi et al. [13] analyzed the behavior of AA5182-O and DP600 steel sheet (1mm thick) in EHF. The tests were conducted on free forming of sheet metal in a conical die to measure deformation of the sheet metal from its initial value, velocities of sheet metal along z-direction and strain along x- direction at different applied energies.

Automobile industries aim to reduce the fuel consumption by reducing the weight of the components. Lightweight materials such as Al, Cu, Mg can be used to reduce weight of components as compared to other materials [14, 15], but they exhibit low formability. The high strain rate forming provides solution to these sheet metal problems [16]. Electrohydraulic forming is a high strain rate forming method, which can be studied to enhance formability of lightweight materials.

The present problem targets to study the deformation behavior of commercially available Aluminum AA1100 sheets in EHF process. The optimization of process parameters and their effect on the process capability has also been assessed using statistics method like Taguchi. Annealed Aluminum sheet of thickness 0.25 mm was used and the chemical composition is shown in Table 1. The tensile tests of annealed samples were carried out on a UTM. In transverse direction, the sample has an Ultimate Tensile Stress of 85 MPa at 10 % elongation. In rolling direction, the sample showed higher ultimate tensile strength (100 MPa at 12 % elongation).

Table 1: Chemical composition of commercially available Aluminum (AA1100)

	Chemical composition (% wt)							
Elements	Si	Fe	Cu	Mn	Mg	Zn	other	Al
Percentage weight	0.554	0.948	0.227	0.225	0.03	0.233	0.183	Remaining

2. Experimental setup and importance of process parameters in EHF

The main components of Electrohydraulic forming setup include capacitor bank, charging unit, forming die and high voltage switch. In the present work an impulse magnetizer system of walker make has been used. Twelve capacitors arranged in the form of bank that has a capacitance of 1000 µf and the thyristor is used as high voltage switch. The other instruments used to obtain data include controller, Rogowski Probe, Oscilloscope, LCR (Inductance, Capacitance, and Resistance) and computer for data acquisition. A schematic of various instruments of the total setup is shown in Figure 2(a). The electrodes were connected by a thin copper wire of 0.54mm diameter, which gets exploded (fused at multiple points) due to high energy passing through thin wire. This creates a shock wave in the fluid medium. Air, Water and Oil are selected as the media for the study.

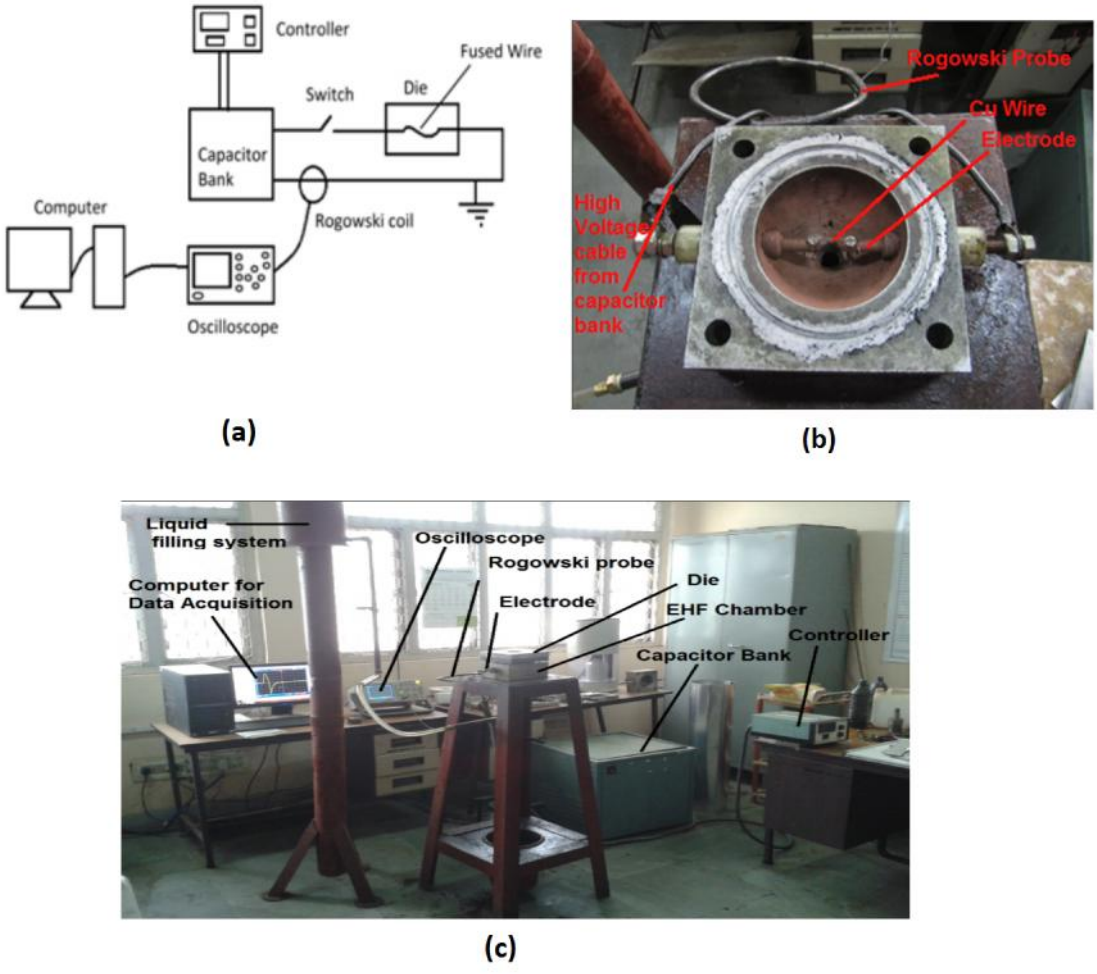

Figure 2: (a) Schematic diagram of full setup (b) Arrangement of electrodes in the chamber and (c) full setup of EHF

The maximum energy that can be discharged from the capacitor bank is 5.25 KJ. The amount of energy discharged by the capacitor bank can be controlled by the controller by setting the voltage. The Rogowski coil is attached to the system circuit as shown in Figure 2(b) and it is used to capture pulse data by storing it through oscillator. The die electrodes and controller are connected by the capacitor bank through high voltage switch**.** Controller is used to regulate and initiate the discharging of the capacitor bank.

The chamber assembly and the complete experimental setup are shown in Figure 2(b) and Figure 2(c) respectively. The copper electrodes are mounted on the opposite face of the hemi spherical cavity. They are insulated from the die by inserting a nylon cylindrical pad. The blank is then kept on the chamber and then clamped by the upper die using four bolts. As the blank is clamped from all the sides, it undergoes biaxial stretching. The free forming die allow blank to deform freely through a cavity of 50 mm diameter. The maximum free bulge height that a blank can achieve before failure represents as limiting dome height (LDH). Limiting dome height and maximum strain that a material can achieve up to necking or failure are the indication of formability in biaxial stretching. Circular grid patterns of 5 mm diameter were prepared on the blank to measure the strains on the blank.

The process parameters need to be optimized to maximize formability of sheet metal. In the present experimental study, Stand-off Distance (SOD) i.e. the distance between the electrodes and the sheet, Gap between electrodes, Voltage and Medium have been considered for optimization to maximize LDH. The control factors and their levels are listed in Table 2. The levels of parameters were decided based on the trial runs of experiments.

Table 2: Control factors and their levels

Control factor	Symbol for coded value	Number of levels		
		1	2	3
Stand-off distance	A	10mm	20mm	30mm
Electrode Gap	B	20mm	30mm	40mm
Voltage	C	220 V	260 V	300 V
Medium	D	Water	oil	air

3. Design of Experiments

An experimental design with four control factors and three levels each will give 81 no. of experiments in full factorial design. To reduce the number of experiments, Taguchi L9 array was used to design the experiments as shown in Table 3. Two samples were tested for each experimental condition to account for uncertainty in the results.

Some tested samples are shown in Figure 3. The measurements of dome height and peak strain on the sample are done using digital micrometer and these are listed in Table 3.

Table 3: Measurements of dome height and peak strain for different experimental conditions

Exp. No.	SOD (mm)	Gap (mm)	Voltage (V)	Medium	Dome height (mm)		Peak strain		S/N Ratio for Dome height	S/N Ratio for Strain
					S 1	S 2	S 1	S 2		
1	10	20	220	Water	3.88	7.03	5.96	4.81	13.63	14.47
2	10	30	260	Oil	7.69	6.36	9.52	5.19	16.81	16.18
3	10	40	300	air	1.66	2.14	1.44	3.37	5.37	5.45
4	20	20	260	air	2.88	2.26	4.13	1.35	8.01	5.15
5	20	30	300	water	8.20	7.72	12.12	12.69	18.00	21.86
6	20	40	220	oil	4.91	4.00	6.92	6.35	12.83	16.41
7	30	20	300	oil	9.81	9.99	14.81	11.83	19.90	22.32
8	30	30	220	air	1.31	0.85	1.92	0.96	0.09	1.70
9	30	40	260	water	5.58	5.93	6.25	5.38	15.18	15.22

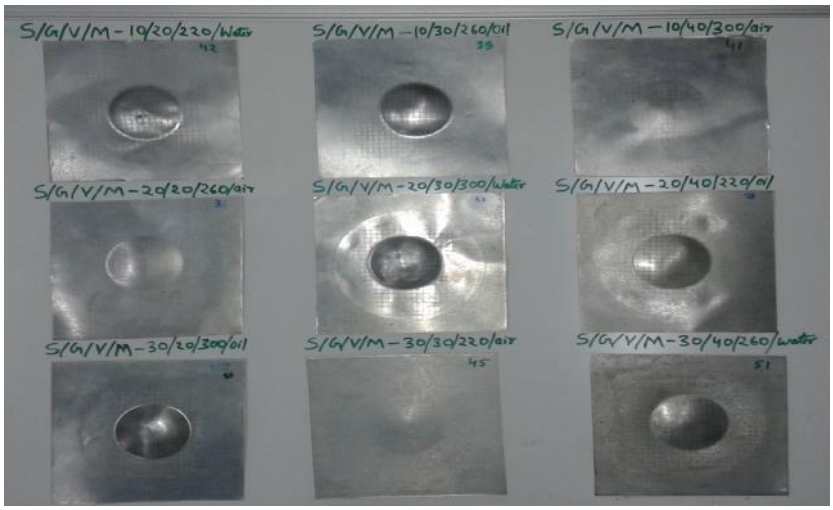

Figure 3: Tested samples in different conditions (S=SOD, G=Electrode GAP, V=Voltage, M=Medium)

The S/N ratio was computed for the dome height and the peak strain separately as per the L9 orthogonal array design of experiments. The objective of maximizing the peak strain is equivalent to maximizing S/N ratio value. Therefore, 'larger the better' criterion is considered for experimental analysis. The combination of process parameters having maximum S/N ratio gives the optimum condition. The mean squared deviation of S/N ratio for a

parameter from the overall mean will give the contribution of individual parameter. Eq. (1) is used to calculate S/N ratio for larger-the better type problem.

$$S/N \ \ ratio\ (\eta) \ = 10 \log_{10} \left[\left(\frac{1}{n}\right) \sum_{i=1}^{n} \frac{1}{y_i^2}\right] \quad (1)$$

where, n is the number of repeat experiments, and y represents the measured value. The S/N ratio for all the experiments conducted is given in Table 3.

The average effect for levels one, two, and three of SOD was computed using data from experimental numbers 1 to 3, 4 to 6, and 7 to 9 respectively. Similarly, the average effect of Gap and Energy was computed for all the levels. The average effect responses were calculated for dome height and peak strain which are shown in Table 4.

Table 4: Average effect response table for the S/N ratio

Dome height	Avg. of η_{SOD}	Avg. of η_{GAP}	Avg. of η_{Energy}	Avg. of η_{medium}
Level 1	12.03	14.64	9.91	15.93
Level 2	13.29	13.46	13.97	16.75
Level 3	13.17	10.39	14.62	5.81
Strain	Avg. of η_{SOD}	Avg. of η_{GAP}	Avg. of η_{Energy}	Avg. of η_{medium}
Level 1	13.59	16.26	12.66	17.70
Level 2	16.93	15.64	15.94	19.11
Level 3	14.18	12.80	16.10	7.90

4 Results and discussion

4.1. Optimization of process parameters

The average of S/N ratios obtained from three different levels for each process variable are plotted in Figure 4 for both peak strain and dome height. Individual graphs are plotted to study the effect of each factor. The behavior of all the control factors on dome height is similar to the case of peak strain. From the average response graph, as the SOD increases the response first increases and then decreases. Initially, when the fusing wire is very close to the sample, the shock wave could not get dispersed on to the sample uniformly, and this may result in lower dome height and peak strain. When the fusing wire is at a large distance from the sample, then the shockwave starts deteriorating itself due to interferences before reaching the sample, thus there exists an optimum condition in between. As the gap between the electrodes decreases, the wave starts from a small confined area and disperses

uniformly in all the directions in the chamber that causes high formability. The energy of the shock wave is directly proportional to the discharged energy by capacitor bank, therefore the dome height and the peak strain increase as the discharged energy increases.

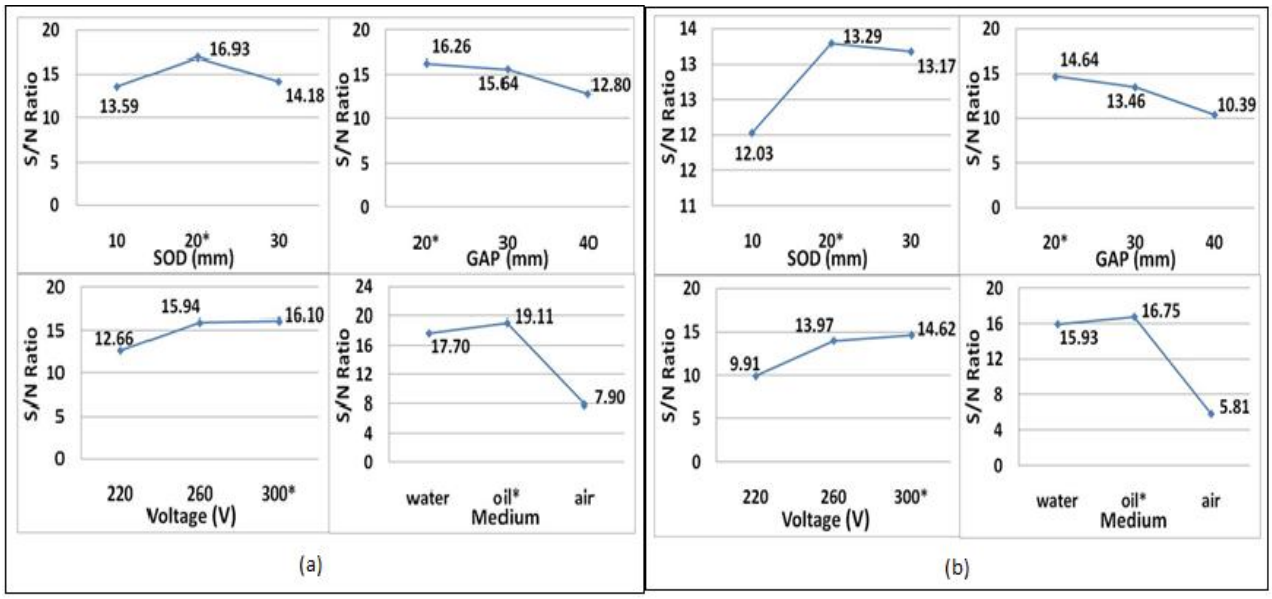

Figure 4: Effect of factor and their levels on S/N ratio for (a) Strain (b) Dome height

From the response plots of all the factors, the optimum levels can be determined by selecting the highest responses of individual factor. Level 2 of SOD has the highest S/N ratio value, which indicates that the performance at such level produces higher strain and dome height. Similarly, level 1 of GAP i.e. 20mm and level 2 of voltage i.e. 260V and level 2 of media i.e. Oil medium have also indicated the optimum condition.

4.2. Calculation for percentage contribution

Different factors affect the strain and dome height to different levels. Therefore, the individual factors must be analyzed to identify the contribution and the effect on the process. The S/N ratio of peak strain in the sheet is used to find the percentage contribution of the control factor process parameters. The average effect response value is used to calculate the sum of squares due to a factor. The sum of squares due to a factor is equal to the total squared deviation for a factor from the overall mean.

$$\text{Sum of squares due to factor} = (l_1 - m)^2 + (l_2 - m)^2 + (l_3 - m)^2 \quad (2)$$

where l_1, l_2, and l_3 are the average effect responses for a factor of level 1, level 2 and level 3 respectively and m is the mean of l_1, l_2, and l_3 . In the above equation, $(l_1 - m)^2$ represents the deviation from the mean value and delta represents the maximum variation in S/N ratio among the control factors at a particular level [17].

$$\text{Percentage contribution of a factor} = \left(\frac{\text{Mean sum of squares due to factor}}{\text{Total mean sum of squars due to all factors}}\right) * 100 \quad (3)$$

Eq. (2) and Eq. (3) are used for calculating sum of squares and percentage contribution respectively for SOD, Gap, Voltage and Medium. The Medium is responsible for a major portion of the variation of S/N ratio i.e. 78% contribution. Similarly, the contribution of other factors can be known, and these are listed in Table 5. The pie chart for the graphical representation of contribution of process parameters is shown in Figure 5.

The larger the contribution of a particular factor to the total sums of squares, the larger the ability of the factor to influence S/N ratio. The larger influence in S/N ratio represents larger influence on control factors. Therefore, in the present case, the effect is maximum on the peak strain due to the media i.e. high density of water and oil when compared with air. Therefore, the large difference in strain causes the medium to contribute maximum when the density difference is high.

Table 5: Percentage contribution of process parameters on peak strain

Process parameters	Degree of freedom	Sum of Square	Mean Sum of square	Contribution (%)	Avg. effect at level			Delta	Rank
					1	2	3		
SOD	2	6.37	3.18	6.69	-0.80	0.46	0.34	1.26	4
GAP	2	6.80	3.40	7.14	1.81	0.63	-2.44	4.25	3
Voltage	2	7.51	3.75	7.88	-2.92	1.13	1.78	4.71	2
Medium	2	74.59	37.29	78.27	3.09	3.92	-7.02	10.94	1
Total	8	95.29	47.64	100.000					

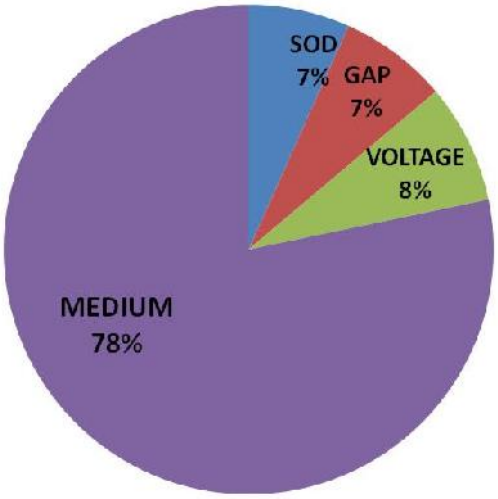

Figure 5: Pie chart to represent the contribution of process parameters

5. Conclusion

Present study is carried out to investigate the forming behaviour of commercial Al sheet at high strain rates through EHF process and optimize the EHF process parameters through a suitable DOE statistical method. Based on the work carried out the following conclusion may be drawn: EHF process for a set of given die and material can be optimized through the established DOE Taguchi method. Taguchi analysis established that the max LDH can be obtained with following combination of parameters: SOD: 20mm, Electrode Gap: 20mm, Medium: Oil/Water, and Energy: 472.5 J / 300 V.

Effect of each process parameter can also be evaluated in terms of percentage using Taguchi method. There is huge effect of density of the medium on the efficiency of the process. Energy, SOD and Electrode Gap also have minor effect on the deformation but cannot be neglected and should be properly optimized.

5. References

[1] Daehn, G.S., Altynova, M., Balanethiram, V.S., Fenton, G., Padmanabhan, M., Tamhane, A., and Winnard, E., (1995), "High-Velocity Metal Forming – An Old Technology Addresses New Problems," JOM, Vol. 7, July 1995, pp. 42-45.

[2] Bruno, E.J. (1968), “High-velocity forming of metals”, American Society of Tool and Manufacturing Engineers Publication

[3] Ahmed, M., Panthi, S. K., Ramakrishnan, N., Jha, A.K. Yegneswaran, A. H. Dasgupta, R., Ahmed, S. (2010), “An Alternative Flat Coil Design for electromagnetic Forming using FEM”, Trans. Of non-ferrous metal society of China

[4] Golovashchenko, S.F., Gillard, 1, A.J., Mamutov, A.V., (2013) “Formability of dual phase steels in electrohydraulic forming” Journal of Materials Processing Technology, Volume 213, Issue 7, July 2013, pp. 1191–1212 , DOI: 10.1016/j.jmatprotec.2013.01.026

[5] Loeffler, M., Wieland, H.A., Neumann, J., Dreesen, C., (2001), “Electrical Wire Explosions as a Basis for Alternative Blasting Techniques?” International Conference on Pulsed Power Applications Paper Number: E.16 Gelsenkirchen, March 27-29, 2001

[6] Mynors D.J., Zhang B.,(2002) “Applications and capabilities of explosive forming”, Journal of Materials Processing Technology, Volumes 125–126, 9 September 2002,

[7] Golovashchenko, S.F., (2006), “Material formability and coil design in electromagnetic forming” Journal of materials engineering and performance, Volume 16, issue 3, June 2007, pp.314-319, DOI: 10.1007/s11665-007-9058-7

[8] Yutin, L. A. (1955), “Electrohydraulic effect”, Mashgiz, Moscow (state scientific technical press for machine construction Literature), translation No.-AD-267-722, armed services technical information agency, Arlington hall station, Arlington, Va., pp. 5–22.

[9] Wesley, R. (1963), "Principles of Electrospark Forming", SAE Technical Paper 630026, doi:10.4271/630026.

[10] Schwinghamer, R. (1964), "Electrical and Diagnostic Aspects of Electrohydraulic and Magnetic Forming", SAE Technical Paper 640002, 1964, doi: 10.4271/640002.

[11] Gilchrist, L., Crossland, B. (1967), “The forming of sheet metal using an underwater electrical discharge”, Proceeding of the conference on electrical methods of machining and forming, publication No. 38, Pages 92-113

[12] Farzin, M., Montazerolg, H., (2009), “Manufacture of thin miniature parts using Electrohydraulic forming and Viscous pressure forming methods”, Archives of metallurgy and materials, Volume 54, Issue 2

[13] Rohatgi, A., Soulami, A., Stephens, E.V., Davies, R.W., Smith, M.T. (2013), “An Investigation of Enhanced Formability in AA5182-O Al During High-Rate Free-Forming at Room-Temperature: Quantification of Deformation History”, Journal of Materials Processing Technology, Available online 31 July 2013

[14] Cole, G.S., Sherman, A.M.,(1995) “Light weight materials for automotive applications”, Materials Characterization, Volume 35, Issue 1, Microstructural Characterization of Lightweight Structural Materials Transportation, July 1995, pp. 3–9, DOI: 10.1016/1044-5803(95)00063-1

[15] Immarigeon, J.P., Holt, R.T., Koul, A.K., Zhao, L., Wallace, W., Beddoes, J.C., (1995), “Lightweight materials for aircraft applications” Materials Characterization, Microstructural Characterization of Lightweight Structural Materials Transportation, Volume 35, Issue 1, July 1995, pp. 41–67,

[16] Knyazyev, M., Zhovnovatyuk, Y. (2011), “Application of manufacturing techniques at electrohydraulic forming of sheet components with complicated local elements”, Metal 2011, May, 18 – 20, 2011, Brno, Czech Republic, EU

[17] Phadke, M.S., (1989), “Quality engineering using robust design”, AT&T Bell laboratories, Prentice-Hall, Inc publication, ISBN 0-13-745167-9